SNRU Journal of Science and Technology

Journal home page: snrujst.snru.ac.th

Behavior of $xSbNbO_4$ additive $(1-x)Ba(Zr_{0.2}Ti_{0.8})O_3$ ceramics with ferroelectric properties

Wattana Photankham[1,*], Hussakorn Wattanasarn[2], Nattee Khottummee[1], Kunchit Singsoog[1]
[1]Center of Excellence on Alternative Energy, Research and development institution, Sakon Nakhon Rajabhat University, 47000 Thailand.
[2]Program of Physics, Faculty of Science and Technology, Sakon Nakhon Rajabhat University, 47000 Thailand.
[*]**Corresponding Author**: w_photankham@hotmail.com

Received: 5 August 2020; **Revised**: 30 October 2020; **Accepted**: 5 November 2020; **Available online**: 1 January 2021

Abstract

$(1-x)Ba(Zr_{0.2}Ti_{0.8})O_3$-$xSbNbO_4$ ceramics were synthesized by the solid state reaction method to examine the crystalline structure, and dielectric and ferroelectric properties of the samples. XRD patterns exhibited the microstructure and tetragonal phase for all samples with sintering temperature at 1150 ºC. The results showed that 1 mol% $SbNbO_4$ coexisted between the tetragonal and cubic phases. The dielectric constant was increased by adding $SbNbO_4$ for 3 mol%, while the dielectric loss decreased slightly. The *P-E* loops showed normal ferroelectric and relaxor ferroelectric behavior. In addition, the good ferroelectric properties exhibited E_c = 2.80 kV·cm^{-1} and P_r = 7.24 μC·cm^{-2} for 4 mol% $SbNbO_4$ which originated to the Perovskite structure tetragonal phase.

Keywords: Microstructure; Dielectric properties; Polarizability; Solid state reaction

1. Introduction

$Ba(Zr_{0.2}Ti_{0.8})O_3$ is a ferroelectric material with a perovskite-type structure (ABO_3) [1]. Ferroelectric materials are used for development in the electronic industry, such as sensors, dielectric amplifiers, detectors, capacitors and multilayer ceramic capacitors (MLCC) [2]. Today, ferroelectric materials are popular topics of research. This is partly due to concerns of PbO toxicity. Research on lead-free piezoelectric ceramics with excellent properties have been replaced in recent years [3]. $Ba(Zr_{0.2}Ti_{0.8})O_3$ exhibit a high dielectric constant (ε_r) at about 1,400 [2 – 9], lower dielectric loss [4 – 9], a remnant polarization (P_r) at about 13.5 kV·cm^{-1} [4,6], coercive field (E_c) of about 2.9 kV cm^{-1} [6], density of about 6.02 g·cm^{-3} [4, 10] and grain size at about ~1 μm [4 – 10]. However, the properties of $SbNbO_4$ are inferior to the $Ba(Zr_{0.2}Ti_{0.8})O_3$ (BZT) system. Several researchers have studied additions to composites, such as $xBaZrO_3$-$(1-x)BaTiO_3$ [3], $Ba(Zr_xTi_{1-x})O_3$ [4], xCa-$xBaTiO_3$ [5], xAl-$xBaTiO_3$ [6] and BZT15/85 [10]. Recently, fine grains of approximately 1 μm have been reported as the piezoelectric properties for the $Ba(Zr_{0.2}Ti_{0.8})O_3$ system. Thus, for the property enhancements of the microstructure to be optimal, the synthesized method is required. Also, importantly, the dopant could greatly support the piezoelectric properties. Among dopant, $SbNbO_4$ is a good material because it is abundant and inexpensive [9]. It also has good piezoelectric properties, with a decrease in the sintering temperature. $SbNbO_4$ is one of the materials that exhibits semiconducting and piezoelectric properties [9]. Recently, it has been used in a wide range to enhance the piezoelectric properties such as d_{33} and k_p included grain growth [9, 10].

Thus, in this paper, we present the synthesized (1-x)$Ba(Zr_{0.2}Ti_{0.8})O_3$-x$SbNbO_4$ composite that was conducted under different conditions by the solid state reaction method. The effects of adding $SbNbO_4$, including the physical and ferroelectric properties for enhanced ferroelectric properties, were systematically studied.

2. Materials and methods

(1-x)$Ba(Zr_{0.2}Ti_{0.8})O_3$-x$SbNbO_4$ systems were synthesized by the solid state reaction method with compositions of x = 1, 2, 3, 4 and 5 mol%. The high-purity precursor powder [composed of $BaCO_3$ (99%), ZrO_3 (99%), TiO_2 (99%), Sb_2O_5(98%), and Nb_2O_3(99.9%)] was used for the formula of (1-x)$Ba(Zr_{0.2}Ti_{0.8})O_3$-x$SbNbO_4$. Both $Ba(Zr_{0.2}Ti_{0.8})O_3$ and $SbNbO_4$ were synthesized with the separated term in which $Ba(Zr_{0.2}Ti_{0.8})O_3$ and $SbNbO_4$ were mixed at a ratio of Ba:(Zr:Ti) = 1:(0.5:0.5) and Sb:Nb = 1:1 into a zirconia ball, milled in deionized water for 24 h, and then volatilized. Then, they were calcined at 830 °C for 4 h and subsequently mashed. The powders were obtained by varying the fraction x as (1-x)$Ba(Zr_{0.2}Ti_{0.8})O_3$-x$SbNbO_4$. After that, the compounds were mixed into a zirconia ball milled in deionized water for 24 h, and then the volatilization. These powers were calcined at 830 °C for 4 h and mashed. The composition of the (1-x)$Ba(Zr_{0.2}Ti_{0.8})O_3$-x$SbNbO_4$ was mixed PVA and uniaxially pressurized under 320 MPa into the mold to disc samples. The condition of sintering temperature at 1,150 °C with a heating rate of 10 °C·min^{-1} under atmospheric for 2 h, then soaked and cooled to room temperature. The investigation used crystal structures with x-ray diffraction technique (Shimadzu XRD-6100), where the diffraction intensity was measured in a range between 20° to 70° with a step-up of 0.02°. ferroelectric properties, disc samples were obtained by coating the two main surfaces with silver paint for poling treatment, hysteresis loop and dielectric constant measurement. The dielectric measurement was conducted at 30 to 300°C,using a Chen Hwa 1061 LCR-Meter. The capacitance was determined by $\varepsilon_r = \frac{Ct}{\varepsilon_0 A}$ (ε_r is dielectric constant, C is capacitance, t is thickness, ε_0 is permittivity of a vacuum, A is area).

3. Results and Discussion

Physical Properties

The XRD patterns of (1-x)$Ba(Zr_{0.2}Ti_{0.8})O_3$-x$SbNbO_4$ with the composition of 1, 2, 3, 4 and 5 mol% are shown in Fig. 1. The tetragonal (P4mm) phase structure of all samples is seen in Fig. 1(a). It is evident that the major phase is (1-x)$Ba(Zr_{0.2}Ti_{0.8})O_3$-x$SbNbO_4$, following the existing of $Ba_6Ti_{17}O_{40}$ and $BaTi_2O_5$ phases (showing as a cubic phase). The diffraction peaks of the tetragonal system (P4mm) could be indexed as perovskite structures in the XRD graphs [1, 3]. The samples showed the ferroelectric perovskite phases coexisted between the tetragonal to pseudo (cubic) phases. Fig. 1(b), The splitting peaks between $(002)_T$ and $(200)_T$ indicated the tetragonality of *c/a* with zoomed 2θ rang 44 – 46°, conformed by the percentage of tetragonality, which was observed by the change of $(002)_T$ and $(200)_T$ peaks in Fig. 1 (b). Thus, the $SbNbO_4$ content increased with influence to lattice parameter *a* increases, *c* decreases; hence, the tetragonal (*c/a*) distortion increased, as shown in Fig. 2. The abnormal tetragonality was lowest in the 1 mol% sample because the $(002)_T$ and $(200)_T$ peaks appear with coexisting as shown in Fig. 1(b) [1, 3, 9]. In contrast, the 4 mol% sample obtained high tetragonality were split at $(200)_T$. Thus, the results of XRD assume that the added 2 mol% may be near Morphotropic Phase Boundaries (MPB phase), which indicates that an overlap of the structures has a negative impact on symmetry, with good ferroelectric properties [12]. When $SbNbO_4$ content was further increased, there were visible affirm with increases of $(002)_T$ and $(200)_T$, supplementary in percentage tetragonality. At more

than 3 mol% content, the tetragonal phases became dominant in the (1-x)$Ba(Zr_{0.2}Ti_{0.8})O_3$-x$SbNbO_4$ as x increased. Generally, the incorporation of elements for the site in the (1-x)$Ba(Zr_{0.2}Ti_{0.8})O_3$-x$SbNbO_4$ perovskite structure can be predicted by considering the corresponding ionic radii and the Goldschmidt tolerance factor $t = \frac{r_A + r_O}{\sqrt{2}(r_B + r_O)}$ [15]. The tolerance factor obtained incorporation the ionic radii of Ba^{2+}(1.35 Å), Ti^{4+}(0.745 Å), Zr^{2+}(0.74 Å) and O^{2-}(1.4 Å), the *t* value is 0.906 of (1-x)$Ba(Zr_{0.2}Ti_{0.8})O_3$-x$SbNbO_4$. Therefore, the substitution of Zr^{2+} may occur more in B site [9] that the *t* of B-site (Ti) substitution in this doping is close to 1; therefore, B site substituting is more likely to occur).

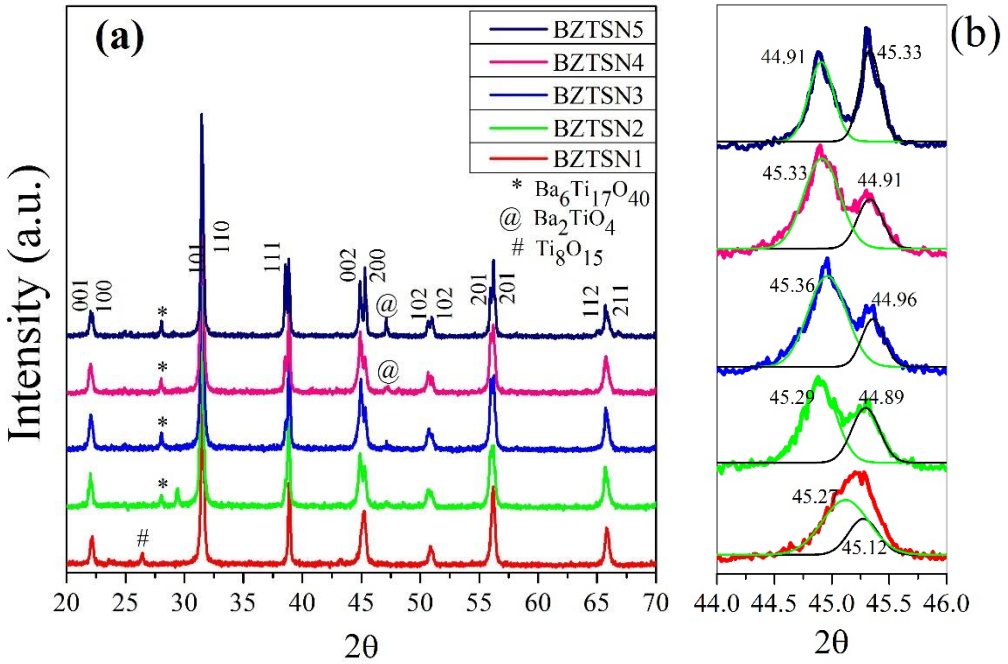

Fig. 1 (a) XRD patterns of the (1-x)$Ba(Zr_{0.2}Ti_{0.8})O_3$-x$SbNbO_4$ (BZTSN) with x=1, 2, 3, 4 and 5 mol% and sintering at 1150 °C. (b) Enlarged XRD graph of zoom rang 44 – 46°.

Table 1 ferroelectric properties of the (1-x)$Ba(Zr_{0.2}Ti_{0.8})O_3$-x$SbNbO_4$ (BZTSN)ceramics.

samples	Perovskite phase (%)	Dielectric constant (ε_r)	Temperature max (°C)	P_r ($\mu C \cdot cm^{-2}$)	(E_c) ($kV \cdot cm^{-1}$)
BZTSN1	95.30	722	176	13.38	7.24
BZTSN2	72.68	829	180	1.23	1.00
BZTSN3	86.28	767	184	7.63	5.05
BZTSN4	84.72	1038	188	7.24	2.80
BZTSN5	91.83	908	188	12.89	4.68

Table 1 shows the ferroelectric properties of the (1-x)$Ba(Zr_{0.2}Ti_{0.8})O_3$-x$SbNbO_4$ ceramics. It was found that the perovskite phases reached a maximum of 1 mol% (about 95.30), with opine the carbon atoms have lower concentration which non-perovskite structure [1,9,10]. Moreover, as the lattice parameter decreases, c increases, which also increases tetragonality (*c/a*). The tetragonality *c/a* of these ceramics obtained decreased when the $SbNbO_4$ content increased, but the Ba^{2+} and Ti^{4+} cations were also enhanced, as shown in Fig. 2. This *c/a* ratio changed when the composite concentration increased. In the 2 mol% sample, the *c/a* ratio increased at 1.0159 and then the *c/a* ratio decreased at 1.0079 added composites ample to 3 mol.%. Therefore, the Bragg angle of appeared splitting several peaks to percentage perovskite phase increases was more than 85%, as

shown in Table 1. The relations of ferroelectric properties were $Ba(Zr_{0.2}Ti_{0.8})O_3$-$xSbNbO_4$ ceramics, with sintering at 1,150 ºC for 2 h. The dielectric properties exhibit with a direct relationship between ε_r on T_{max} which increased with the addition of SbNbO content; meanwhile the E_c present increased as listed in Table 1. It was observed that the 4 mol% sample shows significantly different ε_r and E_c, regarding with Sb^{2+} and Nb^{2+} ions affecting the dielectric properties, within the conductivity of behavioral ceramics. SbNbO content into samples ceramics was attempt modified on dielectric property, Sb^{2+} and Nb^{2+} seriously helpful to adjust electrical properties [9]. Interestingly, with 5 mol% $SbNbO_4$, the dielectric loss increased remarkably, and the dielectric constant decreased. However, a report corresponding to Soma Chattopadhyay et al., stated that Sb and Nb have good dielectric properties [9]; the dielectric loss increased rapidly, but the dielectric constant decreased. From *P–E* hysteresis loops for the (1-x)$Ba(Zr_{0.2}Ti_{0.8})O_3$-$xSbNbO_4$ ceramics with different $SbNbO_4$ contents, the evolution data of P_r and E_c as functions of $SbNbO_4$ content are listed in Table 1. P_r and E_c reach their maximum with the increase of 1 mol% and then decreased rapidly with an increase of 2 mol%. In further addition, P_r obtains further increases value about 7.63, 7.24 and 12.89 $kV{\cdot}cm^{-1}$. Fig. 2 for 3, 4 and 5 mol%, respectively. For the $SbNbO_4$ addition, these samples were sintered with an increase in grain growth, since it has been reported that grain size reduces the orientation of polarization along electric fields [9], thus ferroelectric properties have been influenced untroubled. Although 2 mol% exhibited significantly high values, with character *P-E* loops showing normal ferroelectric behavior, regularly exhibited relaxor ferroelectric behavior for BZT [10] indicated a complex perovskite phase. Table 1 shows the remnant polarization (P_r) and coercive field (E_c) for the (1-x)$Ba(Zr_{0.2}Ti_{0.8})O_3$-$xSbNbO_4$ at different mol% content. 5 mol% showed a higher value at around 12.11 $kV{\cdot}cm^{-1}$, while low the at 3.80 $kV{\cdot}cm^{-1}$. Moreover, their samples revealed good values with 2.80 and 4.68 $kV{\cdot}cm^{-1}$ for 4 and 5 mol%, respectively. This result indicated that the ceramic obtain expedient to pole and effect has higher piezoelectric properties.

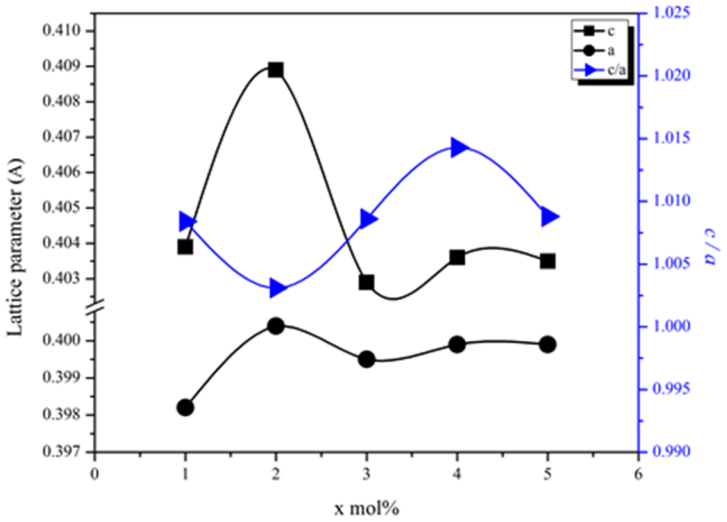

Fig. 2 The lattice parameters of the (1-x)$Ba(Zr_{0.2}Ti_{0.8})O_3$-$xSbNbO_4$ ceramics.

Dielectric Properties

The dielectric constant and dielectric loss of (1-x)$Ba(Zr_{0.2}Ti_{0.8})O_3$-$xSbNbO_4$ adding x with 1, 2, 3, 4 and 5 mol% are shown in Fig. 3. The dielectric behavior is favored to explain the switching domain in micro and nano regions which affect phase transition at different temperatures. Dielectric constant (ε_r) and dielectric loss ($\tan\delta$) as a function of temperature at various frequencies of (1-x)$Ba(Zr_{0.2}Ti_{0.8})O_3$-$xSbNbO_4$ have been obtained. The maximum dielectric constant at

temperature (T_{max}) ranged from 92 – 200ºC for these samples, as seen in in Table 1. Fig. 3 shows the increase of added $SbNbO_4$ content increasing, because of higher capacitance for $SbNbO_4$. But, 2 mol% $SbNbO_4$ has been the ε_r leaked higher at frequency 1 kHz. Meanwhile, x = 3 mol% decreased in this high temperature. Besides, $SbNbO_4$ the broaden peak of ε_r exhibited dispersion, which raised with increasing temperatures at the various frequencies, as given in Fig. 3. The was found raised because pinning domain occurred by Zr^{2+} such domain wall that could not be switching. While added both the $SbNbO_4$, the broaden peak of exhibited distribution which raised when the increasing temperature at a various frequency as give in Fig. 3(a). The of (1-x)$Ba(Zr_{0.2}Ti_{0.8})O_3$-x$SbNbO_4$ 4 mol% was found shift to have the maximum dielectric constant at temperature (T_{max}) from 30 – 300 °C with 176, 180, 184, 188 and 188 °C for x = 1, 2, 3, 4 and 5 mol%, respectively [see in Fig. 3]. Generally, the BZT base showed a maximum dielectric constant of about 123 °C [1, 2, 9]. All samples exhibited a diffuse ferroelectric phase transition with a transition temperature that caused the substitution of $SbNbO_4$ into the O site and Zr^{2+} ions into the B site leading to disorder of complex perovskite structure.

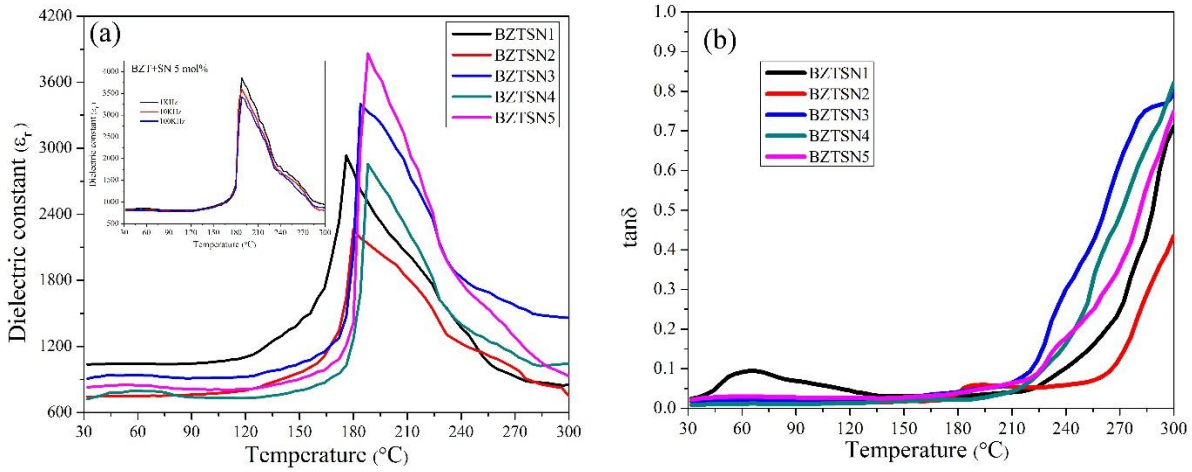

Fig. 3 Dielectric Properties of (1-x)$Ba(Zr_{0.2}Ti_{0.8})O_3$-x$SbNbO_4$ sintering at 1,150°C.

Ferroelectrics

The measurement of the polarization-electric field (*P–E*) hysteresis loops was performed to examine the ferroelectric properties of (1-x)$Ba(Zr_{0.2}Ti_{0.8})O_3$-x$SbNbO_4$ ceramics. Fig. 4 displays the different *P–E* hysteresis loop shapes which can be used to indicate ferroelectric behavior with ceramic composition at room temperature. *P-E* loop of 2 mol% $SbNbO_4$ ceramic was squareness given in Fig. 4. The coercive field (E_c), remnant polarization (P_r), spontaneous polarization (P_s) sharpness of points, and squareness of loop indicated normal ferroelectric behavior. Moreover, it exhibits increasing the domain size and dipoles. The ferroelectric (FE) state displays disruption by the zirconium-titanate (Zr, Ti), which may be a consequence of FE-AFE transformation at high temperatures [13, 15]. While 2 mol% $SbNbO_4$ gave as a flat loop with rapidly lower for P_r, and E_c. These results decreased the ferroelectric domain size, which indicates nanodomains in relaxor ferroelectrics decreases the spontaneous polarization. Nonetheless, with further addition, relaxer ferroelectric behavior has emerged for 3, 4 and 5 mol%. These include ferroelectric domain size increasing to microdomains along with E_c, P_r and P_s, as depicted in Fig. 4.

Fig. 4 shows characteristics of the polarization-electric field (*P-E*) hysteresis loops of (1-x)$Ba(Zr_{0.2}Ti_{0.8})O_3$-x$SbNbO_4$ ceramics at room temperature. All samples possess ferroelectric behavior from the *P-E* hysteresis loop. The characteristic of *P-E* hysteresis loops exhibited relaxor ferroelectric behavior, indicating to the domain size. In the 3 mol% sample, it observing attempt

in change ferroelectric behavior, cause of $SbNbO_4$ substituted due to the B-site of Ti^{4+}. Therefore, the behavior decreased the spontaneous polarization (P_s), as displayed in Fig. 4. Thus, the domain size rapidly decreased and then increased with the content of 4 mol%. Fig. 4, illustrates several the remnant polarizations (P_r) and coercive fields for the (1-x)$Ba(Zr_{0.2}Ti_{0.8})O_3$-x$SbNbO_4$ at different contents. The BZT shows a higher value at around 12.11 kV·cm^{-1}, while low at 3.8 kV·cm^{-1}. With 4 and 5 mol% added, the samples exhibited high values of 14.86 and 15.49 kV·cm^{-1} Fig. 4, respectively. Moreover, their samples obtained good values with 1.79 and 2.13 kV·cm^{-1} for 4 and 5 mol% content, respectively. This result indicates that the ceramic obtain expedient to pole and effect has higher piezoelectric properties.

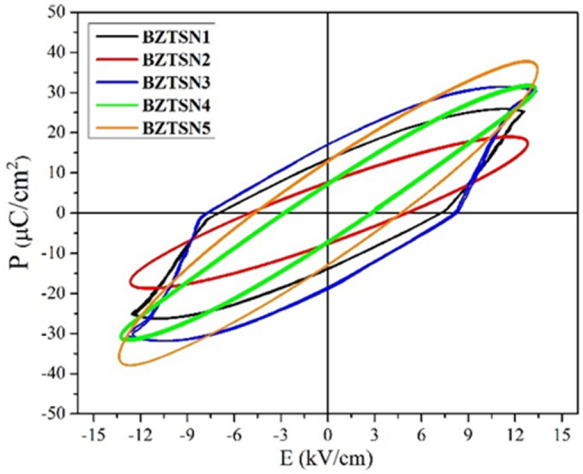

Fig. 4 *P-E* hysteresis loop of (1-x)$Ba(Zr_{0.2}Ti_{0.8})O_3$-x$SbNbO_4$ sintering at 1,150 °C.

4. Conclusion

The temperature of the dielectric constant maximum (T_{max}) shifted from 180 °C to the 188 °C with increasing $SbNbO_4$ content. While the dielectric constant (ε_r) was further increased at the $SbNbO_4$ contents of 2, 3, and 4 mol%, it decreased with 5 mol% $SbNbO_4$. During the addition of (1-x)$Ba(Zr_{0.2}Ti_{0.8})O_3$-x$SbNbO_4$, when a further amount of $SbNbO_4$ was added to the BZT, the dielectric loss decreased because of capacitance in the $SbNbO_4$ content, but rose at higher temperatures. In $SbNbO_4$ addition, the dielectric property was fabricated electrical conductance of $SbNbO_4$. The dielectric constants slightly decreased, while the dielectric loss increased stability with increased temperature. Moreover, with the addition of (1-x)$Ba(Zr_{0.2}Ti_{0.8})O_3$-x$SbNbO_4$, the *P-E* hysteresis loop became narrower as the $SbNbO_4$ content increased, but displayed normal and relaxor ferroelectric behavior. The formation of $SbNbO_4$ has been enlarged with the reduction of the oxygen vacancy. The ferroelectric properties show a higher remnant polarization (P_r) and coercive field (E_c) at about 13.38 μC·cm^{-2} and 7.24 kV·cm^{-1} for 1 mol%. With the increasing $SbNbO_4$ content, P_r and E_c decreased. The ferroelectric properties of samples exhibited relaxor ferroelectric behavior at room temperature. The electrical properties were good P_r and E_c for 4 and 5 mol% were considered good.

5. Suggestions

The synthesis should be prepared in an inert gas atmosphere. It had the reducing reaction on oxygen for firing $SbNbO_4$.

6. Acknowledgement

This work was supported by the Center of Excellence on Alternative Energy allowing usage of its instruments for measurement.

7. References

[1] X.G.Tang, J.Wang, X.X.Wang, H.L.W.Chan, Effects of grain size on the dielectric properties and tunabilities of sol–gel derived $Ba(Zr_{0.2}Ti_{0.8})O_3$ ceramics, Solid State Commun. 131 (2004) 163 – 168.

[2] J. Hao, W. Li, J. Zhai, H. Chen, J. Zhai, Progress in high-strain perovskite piezoelectric ceramics. Mater Sci Eng R. 135 (2019) 1 – 57.

[3] L. Dong, D.S. Stone, R.S. Lakes, Enhanced dielectric and piezoelectric properties of $xBaZrO_3$-(1-x)$BaTiO_3$ ceramics, J Appl Phys. 111 (2012) 084107.

[4] L. Xu,Y. Xu, Efect of Zr^{4+} content on crystal structure, micromorphology, ferroelectric and dielectric properties of $Ba(Zr_xTi_{1-x})O_3$ ceramics, J Mater Sci-Mater El. 31 (2020) 5492 – 5498.

[5] X.M. Chen, T. Wang, J. Li, Dielectric characteristics and their field dependence of $(Ba,Ca)TiO_3$ ceramics, Mat Sci Eng B. 113 (2004) 117 – 120.

[6] A.I. Ali, C.W. Ahn, Y.S. Kim, Enhancement of piezoelectric and ferroelectric properties of $BaTiO_3$ ceramics by aluminum doping, Ceram Int. 39 (2013) 6623 – 6629.

[7] S. Wu, X. Wei, X. Wang, H. Yang, S. Gao, Effect of Bi_2O_3 Additive on the Microstructure and Dielectric Properties of $BaTiO_3$-Based Ceramics Sintered at Lower Temperature, J Mater Sci Technol. 26(5) (2010) 472 – 476.

[8] H. Cheng, H. Hida, J. Ouyang, I. Kanno, Electromechanical properties of $BaTiO_3$-x$BaSnO_3$ thin films prepared via combinatorial sputtering, Ceram Int. 43 (2017) 1597 – 1601.

[9] S. Chattopadhyay, P. Ayyu, M. Multani, R. Pinto, Synthesis of oriented thin films of ferroelectric $SbNbO_4$ on Si by pulsed laser ablation, J Appl Phys. 83 (1998) 3911.

[10] M.L.V. Mahesh, V.V.B. Prasad, A.R. James, Enhanced dielectric and ferroelectric properties of lead-free $Ba(Zr_{0.15}Ti_{0.85})O_3$ ceramics compacted by cold isostatic pressing, J Alloy Compd. 611 (2014) 43 – 49.

[11] S. Byeon, J. Yoo, Effects of Zn Substitution on Dielectric and Piezoelectric Properties of $(Na_{0.54}K_{0.46})_{0.96}Li_{0.04}(Nb_{0.90}Ta_{0.10})O_3$ Ceramics, J Appl Phys. 51 (2012) 09MD12.

[12] X. Zhao, W. Chen, L. Zhang, L. Zhong, The effect of the bipolar field on the aging behavior and the associated properties of the Mn-doped $BaTiO_3$ ceramics, J Alloy Compd. 618 (2015) 707 – 711.

[13] Relaxor Behaviour in Ferroelectric Ceramics, https://www.intechopen.com/books/advances-in-ferroelectrics/relaxor-behavior-in-ferroelectric-ceramics, 5 June 2020.

[14] E. Sun, W. Cao, Relaxor-based ferroelectric single crystals: Growth, domain engineering, characterization and applications, Prog Mater Sci. 65 (2014) 124 – 210.

[15] L. Yang, X. Li, E. Allahyarov, P.L. Taylor, Q.M. Zhang, L. Zhu, Novel polymer ferroelectric behavior via crystal isomorphism and the nanoconfinement effect, Polymer. 54 (2013) 1709 – 1728.

[16] C.J. Bartel, C. Sutton, B.R. Goldsmith, R. Ouyang, C.B. Musgrave, L.M. Ghiringhelli, M. Scheffler, New tolerance factor to predict the stability of perovskite oxides and halides, Sci. Adv. 5(2) (2019) eaav0693.